Determination of thermodynamic functions and structural parameters of NpO_2^+ lactate complexes†

M. M. Maiwald, *[a] K. Müller, [b] K. Heim,[b] M. Trumm, [c] N. L. Banik,[d] J. Rothe,[c] K. Dardenne, [c] A. Skerencak Frech[c] and P. J. Panak[ac]

The complexation of NpO_2^+ with lactate in aqueous solution is studied as a function of the total ligand concentration ([Lac]$_{total}$), ionic strength (I_m = 0.5 4.0 mol kg ^{1} Na^+(Cl /ClO_4)) and temperature (T = 20 85 °C) by Vis/NIR absorption spectroscopy. The formation of two NpO_2^+ lactate species with the stoichiometry $NpO_2(Lac)_n^{1\ n}$ (n = 1, 2) is observed at the studied experimental conditions. The temperature dependent conditional stability constants $\log \beta_j'(T)$ at different ionic strengths are calculated with the law of mass action. The conditional data are extrapolated to IUPAC reference state conditions (I_m = 0) with the specific ion interaction theory (SIT). With increasing temperature up to 85 °C $\log \beta_1^0$ (20 °C) = 1.92 ± 0.14 decreases by 0.12 and $\log \beta_2^0$(20 °C) = 2.10 ± 0.13 decreases by 0.17. The thermodynamic stability constants correlate linearly with the reciprocal temperature according to the integrated Van't Hoff equation. Thus, linear regression analyses yield the standard reaction enthalpy $\Delta_r H^0$ and entropy $\Delta_r S^0$ for the complexation reactions. In addition, the sum of the SIT specific binary ion ion interaction coefficients $\Delta\varepsilon_{j,k}(T)$ of the complexation reactions are determined by variation of the ionic strength. Structural parameters of the formed complex species and the coordination mode of lactate towards the NpO_2^+ ion are investigated as a function of pH_c by extended X-ray absorption fine structure spectroscopy (EXAFS) and attenuated total reflection Fourier-transform infrared spectroscopy (ATR-FT IR). The results show, that the coordination mode of lactate changes from end-on (coordination *via* only the COO group) to side-on (formation of chelate rings involving the OH-group) with increasing pH_c. The experiments are supported by quantum chemical calculations.

1 Introduction

Deep geological formations are considered for the final disposal of high-level nuclear waste. Suitable host rock formations discussed in several European countries (*e.g.* Belgium,[1] France,[2] Germany[3] and Switzerland[4]) are rock salt, crystalline formations (*e.g.* granite) and clay rocks. Due to their long half-lives, the transuranium element plutonium (Pu) and the minor actinides (Np, Am) determine the long-term radiotoxicity of the nuclear waste. Therefore, the actinides are of particular interest for the safety case of a nuclear waste repository. In case of a release of radionuclides from the primary containments, a mechanistic understanding of the most relevant interactions (*e.g.* dissolution of the waste matrix and solubility of the radionuclides, sorption and complexation processes, *etc.*) of the radionuclides with the surrounding backfill material, the host rock, and the aquifer components is essential. In particular complexation reactions with naturally occurring inorganic and organic ligands in aqueous solution can significantly affect the mobility and migration of the radionuclides.

Depending on the repository design and host-rock characteristics increased temperatures are expected in the near-field of a nuclear waste repository *e.g.* up to 100 °C for clay rocks and up to 200 °C for salt rocks.[5] Additionally, some clay repository sites exhibit high saline conditions, *e.g.* in Northern Germany the ionic strength of the pore water is above 3.5 mol L^{-1}.[3] It was shown earlier that an increase of the temperature and the ionic strength may have a significant influence on complexation processes with different organic and inorganic components in

[a] *Ruprecht Karls Universitat Heidelberg, Physikalisch Chemisches Institut, Im Neuenheimer Feld 253, D 69120 Heidelberg, Germany. E mail: m.maiwald@pci.uni heidelberg.de*
[b] *Helmholtz Zentrum Dresden Rossendorf, Institut fur Ressourcenokologie, Bautzner Landstraße 400, 01328 Dresden, Germany*
[c] *Karlsruher Institut fur Technologie (KIT), Institut fur Nukleare Entsorgung (INE), D 76344 Eggenstein Leopoldshafen, Germany*
[d] *Joint Research Center JRC Karlsruhe, G.II.6 Nuclear Safeguards and Forensics, European Commission, P.O. Box 2340, D 76125 Karlsruhe, Germany*
† Electronic supplementary information (ESI) available. See DOI: 10.1039/d0nj04291a

natural aquatic systems affecting the retardation efficiency of the host rock.[6] Low-molecular-weight organic compounds (LMWOC) like formate, acetate, propionate, and lactate make up large fractions of the dissolved organic matter in the pore waters of different clay formations (*e.g.* Callovo Oxfordian (Cox) and Opalinus Clay (OPA)).[7–10] Among the LMWOC lactate is only present in concentrations up to [Lac^-] = 17 μM. Thus, lactate will have a minor effect on the (geo)chemical speciation of actinides at environmental conditions but is of particular interest as it provides the possibility to coordinate to the metal ion in different coordination modes.[9,10] This contrasts to mono carboxylic ligands (*e.g.* acetate, propionate) as the lactate molecule can either coordinate end-on *via* the carboxyl function or side-on *via* both the COO^- group and the α-hydroxy group. The coordination mode of lactate might also be affected by the pH value. Thus, lactate can be used as a model ligand to study the effect of α-OH groups in organic compounds on the complex stability, thermodynamic behaviour and structure of An-LMWOC complexes.

Actinides (An) in the pentavalent oxidation state are known to be highly soluble with low retention by mineral phases.[11–17] Within the series of the An(v) the Np(v) ion is the most stable in aqueous solution and is used as an analogue for the An(v) due to its excellent spectroscopic properties.

The present work focusses on the determination of thermodynamic data for the complexation of NpO_2^+ with lactate. Thermodynamic data on NpO_2^+ lactate complexes are scare in the literature and most data are limited to a fixed ionic strength or ambient temperatures. Only one solvent extraction study by Vasiliev *et al.* provides thermodynamic functions ($\Delta_r H^0$, $\Delta_r S^0$, $\Delta\varepsilon_{j,k}(T)$) for the NpO_2(Lac) complex at IUPAC reference state conditions determined from variation of the ionic strength and temperature.[18] In this survey the $\Delta_r H^0$ and $\Delta_r S^0$ values are determined from single point SIT extrapolation at one fixed ionic strength. The effect of the ionic strength on the complexation reaction as a function of the temperature has not been investigated.

Concerning the speciation of the NpO_2^+ lactate complexes different studies based on solvent extraction and spectrophotometry report different results.[18–20] Depending on the experimental approach the formation of only NpO_2(Lac) or both NpO_2(Lac) and $NpO_2(Lac)_2^-$ was observed. Also, the reported conditional stability constants for NpO_2(Lac) differ significantly ($\log \beta'$ (25 °C) = 1.1–1.8, at $I_m(NaClO_4)$ = 1 mol kg^{-1}).

Furthermore, structural investigations are of particular interest as no structural data of An(v)–lactate complexes are available in the literature describing the complexation of An(v) with α-hydroxy carboxylates on a molecular level.

In the present work the complexation of NpO_2^+ with lactate as a function of the ligand concentration, temperature and ionic strength is studied by Vis/NIR absorption spectroscopy. Structural characterization of the complexes is performed by extended x-ray absorption fine structure spectroscopy (EXAFS) and attenuated total reflection Fourier-transform infrared (ATR FT-IR) spectroscopy. The experimental data are supported by quantum chemical calculations.

2 Experimental

2.1 Sample preparation

Caution! ^{237}Np is an α-emitter and must be handled with care in laboratories appropriate for research involving transuranic elements. Health risks caused by radiation exposure or incorporation must be avoided. Higher concentrated Np solutions were handled in glove boxes.

The molal concentration scale (mol kg^{-1} H_2O^{-1} or mol kg_w^{-1}) was used for all solutions to avoid changes of the concentration caused by changes of the temperature or the ionic strength. All chemicals except for neptunium were reagent grade or higher and purchased from Merck Millipore. For sample preparation ultrapure water (Milli-Q academic, Millipore, 18.3 MΩ cm) was used.

2.1.1 Absorption spectroscopy. The total initial NpO_2^+ concentration of all samples used for absorption spectroscopy was adjusted to 2.5 × 10^{-4} mol kg_w^{-1} in 2.1 × 10^{-5} mol kg_w^{-1} $HClO_4$ by dilution of a 4.3 × 10^{-2} mol kg_w^{-1} $^{237}NpO_2^+$ stock solution ($[HClO_4]_{stock}$ = 2.9 × 10^{-3} mol kg_w^{-1}). The preparation of the stock solution is described in the literature.[21] The complexation of NpO_2^+ was studied as a function of $[Lac^-]_{tot}$ at three different ionic strengths (I_m = 0.5, 2.0 and 3.6 mol kg_w^{-1} $Na(ClO_4^-/Lac^-)$) and T = 20 °C ($[Lac^-]_{tot} = [Lac^-]_{eq} + [HLac]_{eq}$; the concentration of the Np(v)–lactate complexes is neglectable for the determination of the complex stoichiometry as $[NpO_2^+] \ll [Lac^-]_{tot}$). The temperature dependence (T = 20–85 °C) of the complexation reactions were determined as a function of $[Lac^-]_{tot}$ at I_m = 3.6 mol kg_w^{-1} $Na(ClO_4^-/Lac^-)$. For preparation of the lactate titration solutions solid sodium lactate was dissolved in water and the ionic strength was adjusted by addition of solid $NaClO_4 \cdot H_2O$. The ionic strength dependence of the complexation reactions was studied in NaCl and $NaClO_4$ media at two fixed ligand concentrations ($[Lac^-]_{tot}$ = 5.7 × 10^{-1}; 3.5 × 10^{-2} mol kg_w^{-1}) between 20 and 85 °C at 8 different ionic strengths between 0.5–4.0 mol kg_w^{-1} NaCl/$NaClO_4$. The concentration of $NaClO_4$ was increased by successive titration using an aqueous 14.5 mol kg_w^{-1} $NaClO_4$ solution. The $[NaCl]_{tot}$ was increased by addition of solid NaCl to the samples. All sample and titration solutions were set to a constant total proton concentration $[H^+]_{tot}$ = 2.3 × 10^{-5} mol kg_w^{-1} using a 0.01 mol kg_w^{-1} $HClO_4$ or HCl ($[H^+]_{tot} = [H^+]_{eq} + [HLac]_{eq}$). As all total proton concentrations are known measurement of the pH values is not necessary. The proton concentrations are calculated using the SIT, integrated Van't Hoff equation and Henderson–Hasselbalch equation (see section "Peak deconvolution and Speciation").

2.1.2 EXAFS spectroscopy. For EXAFS measurements samples with a total NpO_2^+ concentration of 5.0 × 10^{-3} mol kg^{-1} and a concentration of $[Lac^-]_{tot}$ = 2.5 × 10^{-1} mol kg_w^{-1} in H_2O were prepared. The ionic strength of all samples was adjusted to $I_m(Na^+,Lac^-/Cl^-)$ = 4.4 mol kg_w^{-1} by addition of solid NaCl. The EXAFS experiments were conducted at various proton concentrations. The conditional pH_c values (pH_c = 2.6–5.0) were adjusted by addition of small aliquots of 6 mol L^{-1} HCl (Merck, suprapure) or freshly prepared 1 mol L^{-1} NaOH (Merck, Titrisol). The pH was measured by a combination pH

electrode (Orion™ PerpHecT™ ROSS™), which was calibrated with pH reference buffer solutions (Merck, pH = 7.00, 5.00, 2.00). Details on the definition of the pH and pH_c value are given in the literature.[22,23] The volume of each sample was 200 μL.

2.1.3 ATR-FT-IR spectroscopy. The characteristic vibrational modes of the NpO_2^+ ion in solution are generally observed in the spectral range below 850 cm^{-1} where strong interferences with modes of the bulk water (H_2O) occur.[24] Therefore, deuterated water (D_2O, Sigma Aldrich, 99.9 atom % D, stored under argon) was used for the samples of the infrared spectroscopic experiments. All samples were prepared under inert gas atmosphere (N_2) to reduce the content of H_2O. The total NpO_2^+ concentration was 1.0×10^{-3} mol kg_w^{-1} and the ionic strength was I_m = 1.0 mol kg_w^{-1} (Na^+,Lac^-/Cl^-). NaCl was used as background electrolyte as it does not absorb light in the infrared region of interest. The total lactate concentration was $[Lac^-]_{tot} = 1.0 \times 10^{-1}$ mol kg_w^{-1}. The pD_c between 2.6 and 4.8 was adjusted by addition of small aliquots of 0.2 or 2 mol L^{-1} DCl and 0.2 mol L^{-1} NaOD in D_2O. For preparation of the respective acids and bases 35 wt% DCl (Sigma Aldrich, 35 wt% in D_2O, ≥99 atom % D) and 40 wt% NaOD (Alfa Aesar, 40 wt% in D_2O, 99.5 atom % D) were used. The pH values of the samples were determined and adjusted using an inoLab pH 720 pH-Meter (WTW, Weilheim, Germany) with a Blue Line 16pH microelectrode (Schott Instruments, Mainz, Germany). The calibration was performed using standard pH buffers (WTW, Weilheim, Germany) in H_2O. The pD_c values were corrected according to pD = pH + 0.4.[25] The NpO_2^+ concentration in the samples and the species distribution of the samples was confirmed by Vis/NIR spectroscopy. A Varian Cary 5G UV/Vis/NIR spectrophotometer was connected to the inert gas glove box *via* optical fibres to enable the characterization of the NpO_2^+ samples inside the glove box.

2.2 Vis/NIR absorption spectroscopy

The complexation of NpO_2^+ with lactate in aqueous solution was studied by NIR/Vis absorption spectroscopy between 20 and 85 °C using a Varian Cary 5G UV/Vis/NIR spectrophotometer. A Lauda Eco E100 thermostatic system was used to control the temperature of the sample holder. The samples were equilibrated for 15 min at each temperature before measurement to ensure thermodynamic equilibrium. The spectra of the samples placed in quartz glass cuvettes (1 cm path length, Hellma Analytics) were recorded between 950–1050 nm with a data interval of 0.1 nm, a scan rate of 60 nm min^{-1} (average accumulation time 0.1 s) and a slit width of 0.7 nm in double beam mode. For reference measurement and baseline correction samples at the same condition but without NpO_2^+ were measured.

The spectra of the single complex species and the stability constants of the Np(v)–lactate complexes are obtained by peak deconvolution and slope analyses of the mole fractions. The methods of peak deconvolution and slope analysis are described elsewhere.[26–28]

All uncertainties of the stability constants $\log \beta_n^0(T)$, enthalpies $\Delta_r H_{n,m}^0$, entropies $\Delta_r S_{n,m}^0$ and SIT binary ion–ion interaction coefficients $\Delta\varepsilon_{j,k}$ determined in the present work are given with a confidence level of 1 α = 0.95.

2.3 EXAFS measurements

Np L_3-egde-EXAFS spectra were measured in fluorescence mode at an angle of 90° to the incident x-ray beam, using a 4 element Si SDD Vortex (SIINT) detector and an additional 1 element Si Vortex-60EX SDD (SIINT) fluorescence detector. The measurements were performed at the INE-Beamline of the *The Karlsruhe Research Accelerator* (KARA, Karlsruhe, Germany) which was equipped with a double-crystal monochromator (DCM; Ge(422) crystal pair) and a collimating and focusing mirror system (Rh-coated silicon mirrors). The flux of the incident beam was detuned in the middle of the scan range to 70% peak intensity. An Ar-filled ionization chamber at ambient pressure was used to measure the intensity I_0 of the incident X-ray beam. All measurements in the EXAFS range were performed at equidistant *k*-steps and an increasing integration time following a $\sqrt[2]{2}$ progression. The measurements were performed at T = 25 °C. The software packages EXAFSPAK, Athena 0.8.056, and Artemis 0.8.012 were used for data evaluation.[29–31] Theoretical scattering phases and amplitudes were calculated with FEFF8.40, using the crystal structures of UO_2 acetate and oxalate after replacement of the U-atom by Np.[32–34] In all cases the k^2- and k^3-weighted raw EXAFS spectra were fitted.

2.4 ATR FT-IR spectroscopy

In situ ATR FT-IR spectroscopic measurements of the formed NpO_2^+ lactate complexes were performed in D_2O. The spectra were measured on a Bruker Vertex 80/v vacuum spectrometer equipped with a mercury cadmium telluride (MCT) detector. The spectra were recorded between 4000 and 600 cm^{-1} and averaged over 256 scans. The spectral resolution was 4 cm^{-1}. The used ATR unit DURA SamplIR II (Smiths Inc.), a horizontal diamond crystal with nine internal reflections on the upper surface and an angle of incidence of 45°, was purged with a current of dry air (dew point < 213 K). An ATR flow cell with a volume of 200 μL was used to ensure adequate background subtraction without external thermal interference. The measurements were based on the principle of reaction-induced infrared difference spectroscopy. Here, infrared spectra of the solvent, the ligand solution and the samples containing NpO_2^+ at equal experimental conditions (pH_c, I_m, temperature) were recorded in single beam mode. Difference spectra were calculated from spectral data of the NpO_2^+ samples subtracting those of the reference samples exhibiting absorption changes caused by the complexation of the NpO_2^+ ion. Parts of the spectra which are unaffected by the complexation of NpO_2^+, the strong absorbing background from the bulk water as well as contributions from the ATR FT-IR accessory and the instrument were eliminated displaying spectral features even due to minimal absorption changes ($\sim 10^{-5}$ OD).

2.5 Quantum chemical calculations

The TURBOMOLE 7.0 program package was used for quantum chemical calculations and structure optimizations of the NpO_2^+

lactate complexes.[35] The $NpO_2(H_2O)_3(Lac)$ and $NpO_2(H_2O)(Lac)_2^-$ complexes with different coordination modes (side-on *vs.* end-on) were optimized on the level of density functional theory (DFT) using the BH-LYP functional due to its better convergence compared to other hybrid-functionals.[35,36] All N, C, and H atoms were described by triple zeta basis sets (def-TZVP) and were treated at the all-electron level. The Np(v) ion was represented by a 60-electron core pseudo-potential (Np, ECP60MWB) with corresponding basis sets.[37] The triplet spin state with two unpaired f-electrons resulting in a spin multiplicity of $S(S + 1) = 2$ was used for all systems. The gas phase energies E_g were computed on MP2 level. Additionally, thermodynamic corrections ($G_{vib} = E_{zp} + H_0$ TS, E_{zp} being the zero-point energy, H_0 and S are the enthalpies and entropies obtained from the calculations of the vibrational modes) and solvation energies G_{solv} (obtained using COSMO, r(Np) = 1.72 Å) were taken into account to obtain a theoretical approximation of the Gibbs free energies $G = E_g + G_{vib} + G_{solv}$.[38–40] As the ligands and the NpO_2^+ ion are charged a second hydration shell consisting of 28 water molecules was added to avoid the charge of the complexes to contact the COSMO cavity. An application of *ab initio* methods to optimize the structures of the NpO_2^+ complexes was not possible as the size of the systems was too big ($N > 100$ atoms) and the computation time was limited.

3 Results and discussion

3.1 Vis/NIR absorption spectroscopy

3.1.1 Absorption spectra. Fig. 1 shows the absorption spectra of NpO_2^+ as a function of the total lactate concentration $[Lac^-]_{tot}$ at T = 20 and 85 °C and I_m = 3.6 mol kg_w^{-1} $NaClO_4$. At 20 °C the absorption band of the NpO_2^+ ion is located at λ_{max} = 979.4 nm (ε = 397 ± 12 L mol^{-1} cm^{-1}). With increasing $[Lac^-]_{tot}$ a bathochromic shift of the absorption spectra is observed. The Full Width at Half Maximum (FWHM) increases from 7.9 to 10.7 nm indicating the formation of NpO_2^+ lactate complex species.

With increasing temperature the absorption band of the NpO_2^+ ion shifts hypsochromically by 1.2 nm to 978.2 nm while the FWHM is unaffected by the temperature. The extinction coefficient decreases to ε = 362 ± 15 L mol^{-1} cm^{-1}. This blue shift is in good agreement to literature data. There, hypsochromic shifts by 1.5–1.9 nm are reported.[41–45] At 85 °C the bathochromic shift observed at increasing ligand concentration is less pronounced compared to 20 °C. This is also reflected by a smaller increase of the FWHM from 7.9 to 10.4 nm. This indicates a reduced complex formation according to an exothermic complexation reaction.

The spectral changes and hypsochromic shifts of the NpO_2^+ ion with increasing temperature are contrary to the bathochromic shift induced by the complexation of NpO_2^+ at increasing $[Lac^-]_{tot}$. The effect of the temperature on the position of the absorption band of the NpO_2^+ ion has been discussed in the literature in detail.[41,42,44,46] Nevertheless, due to this effect, each series of spectra is evaluated separately and single component spectra must be determined for all experimental conditions.

3.1.2 Peak deconvolution and speciation. The spectra of the formed NpO_2^+ lactate complexes are derived *via* subtractive deconvolution of the absorption spectra using the spectrum of the NpO_2^+ aquo ion. The spectra derived in $NaClO_4$ and NaCl media are identical at equal ionic strengths and temperatures. In Fig. 2 the results of the peak deconvolution are presented for 20 and 85 °C in $NaClO_4$ (I_m = 3.6 mol kg_w^{-1}). The absorption band of $NpO_2(Lac)$ is located at λ_{max} = 983.6 nm (ε = 356 ± 12 L mol^{-1} cm^{-1}), indicating a bathochromic shift of 4.2 nm compared to the absorption band of the NpO_2^+ aquo ion. The absorption band of $NpO_2(Lac)_2^-$ is located at λ_{max} = 987.1 nm (ε = 362 ± 18 L mol^{-1} cm^{-1}) and is shifted by 7.7 nm compared to the aquo ion. This shows, that each coordinating lactate ligand induces an average bathochromic shift of approximately 4.0 nm. At 85 °C all single component spectra are hypsochromically shifted by 1.2 nm whereas the integrated absorption coefficients remain constant. Thus, the absorption spectra of all Np(v) species are affected in the same way by changes of the temperature. Furthermore, at 85 °C the single component spectrum of the $NpO_2(Lac)_2^-$ complex could not be determined due to the low absorption intensity of this species and the unfavourable signal to noise ratio.

The deconvolution of the experimental absorption spectra is performed by principle component analyses using the pure

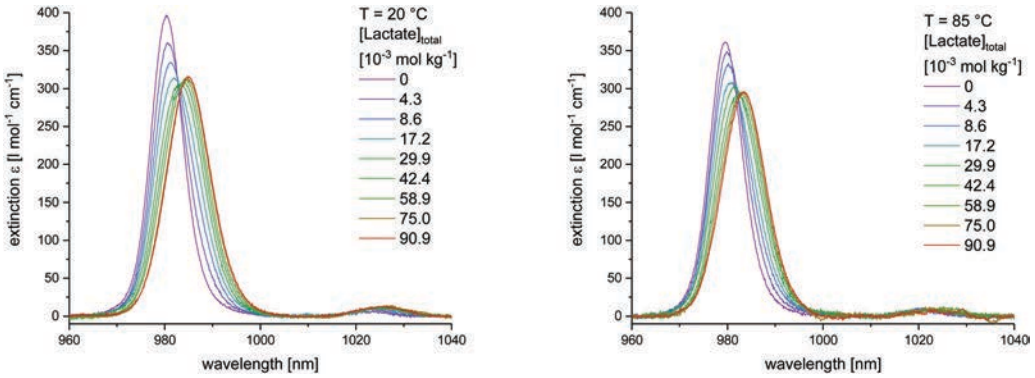

Fig. 1 Absorption spectra of NpO_2^+ with increasing lactate concentration $[Lac^-]_{tot}$ at T = 20 °C (left), and T = 85 °C (right) and I_m ($NaClO_4$) = 3.6 mol kg^{-1}.

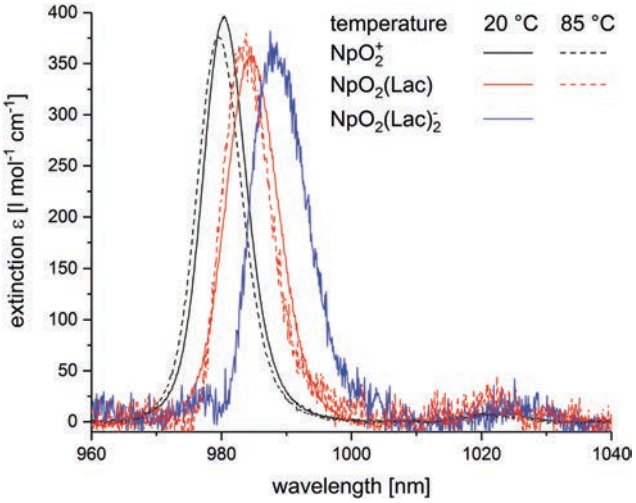

Fig. 2 Absorption spectra of the NpO_2^+ ion and the $NpO_2(Lac)_n^{1-n}$ (n = 1, 2) complexes at T = 20 (lines) and 85 °C (dashed lines) and I_m = 3.6 mol kg_w^{-1} $NaClO_4$.

component spectra. Details on this procedure are given in the literature.[26–28]

The determined speciation of the NpO_2^+ lactate complexation is shown in Fig. 3 (symbols) as a function of the equilibrium lactate concentration $[Lac^-]_{eq.}$ at T = 20 and 85 °C (I_m = 3.6 mol kg_w^{-1} $NaClO_4$). The calculated speciation according to the derived $\log \beta_n'(T)$ values are indicated as solid lines for 20 °C and dashed lines for 85 °C. $[Lac^-]_{eq}$ is calculated at each temperature according to the literature procedure using the Henderson–Hasselbalch equation, SIT and the temperature dependence of the $pK_a^0(H^+ + L^- \rightleftharpoons HL)$ value.[47–49] The required standard reaction enthalpies and protonation constants are given in the literature ($pK_{a,Lac}^0$ = 3.88 ± 0.20; $\Delta_r H_{m,Lac}^0$ = 0.55 ± 0.80 kJ mol^{-1}).[48] For the protonation reaction of Lac^- $\varepsilon(Na^+, Lac^-)$ = 0.01 ± 0.05 is used.[48]

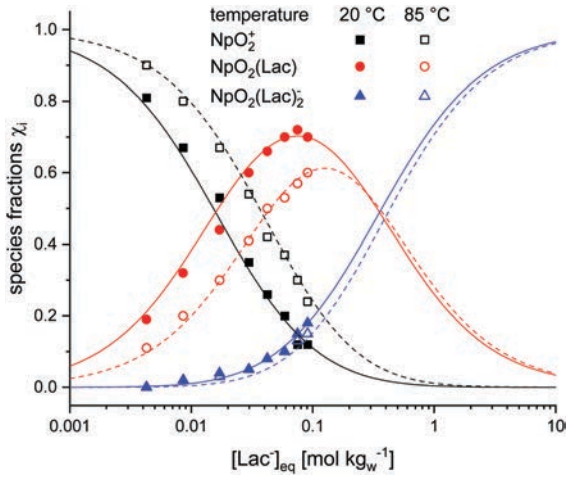

Fig. 3 Experimentally determined (symbols) and calculated species distribution (lines) of $NpO_2(Lac)_n^{1-n}$ (n = 0, 1, 2) complexes as a function of $[Lac^-]_{eq}$ in aqueous solution. I_m = 3.6 mol kg_w^{-1} $NaClO_4$; T = 20 °C (solid lines) and 85 °C (dashed lines).

With increasing ligand concentration, the chemical equilibrium shifts towards the complexed species. For $[Lac^-]_{eq} > 1.6 \times 10^{-2}$ mol kg_w^{-1} the $NpO_2(Lac)$ complex dominates the speciation. The $NpO_2(Lac)_2^-$ complex makes only a minor contribution to the species distribution at the experimental conditions. With increasing temperature the molar fractions of both lactate complexes decrease and the chemical equilibrium shifts towards the NpO_2^+ aquo ion. These trend shows that the complex formation is repressed at elevated temperatures indicating an exothermic complexation reaction of NpO_2^+ with lactate.

3.1.3 Complex stoichiometry. The stoichiometry of the formed complexes is determined by slope analyses at each studied temperature.[26,50] The following complexation model of NpO_2^+ with lactate is applied (eqn (1)).

$$\begin{aligned} NpO_2^+ + Lac^- &\rightleftharpoons NpO_2(Lac) \\ NpO_2(Lac) + Lac^- &\rightleftharpoons NpO_2(Lac)_2^- \\ &\vdots \\ NpO_2(Lac)_{n-1}^{1-(n-1)} + Lac^- &\rightleftharpoons NpO_2(Lac)_n^{1-n} \end{aligned} \quad (1)$$

The slope analyses are performed according to the logarithmic form of the law of mass action (eqn (2)).

$$\log K_n' = \log \frac{[NpO_2(Lac)_n]^{1-n}}{[NpO_2(Lac)_{n-1}]^{1-(n-1)}} \quad 1 \cdot \log[Lac]_{eq}^-; \qquad \beta_n' = \prod K_n' \quad (2)$$

The results of the slope analyses at I_m = 3.6 mol kg_w^{-1} $NaClO_4$ and T = 20 and 85 °C are displayed in Fig. 4. The logarithmic molar fractions $\log \frac{[NpO_2(Lac)_n]^{1-n}}{[NpO_2(Lac)_{n-1}]^{2-n}}$ correlate linearly with $\log[Lac^-]_{eq}$ and linear regression analyses reveal slopes between 0.9 ± 0.1 and 1.1 ± 0.1 for all experimental conditions. Thus, the formation of two NpO_2^+ lactate complexes with a stoichiometry of $NpO_2(Lac)_n^{1-n}$ (n = 1, 2) is confirmed.

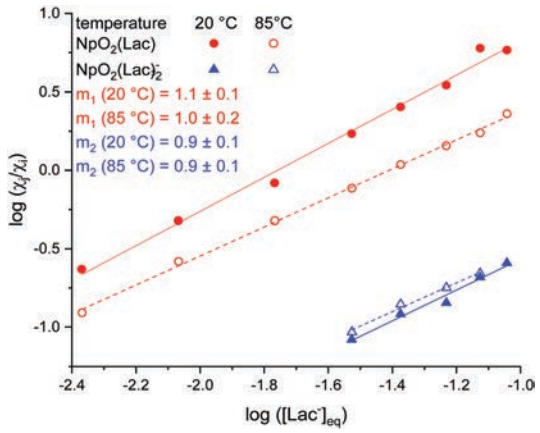

Fig. 4 Plots of log ($[NpO_2(Lac)_n]^{1-n}/[NpO_2(Lac)_{n-1}]^{2-n}$) *vs.* log($[Lac^-]_{eq}$) and linear regression analyses according to eqn (1) at 20 and 85 °C (I_m = 3.6 mol kg_w^{-1} $NaClO_4$).

This result contrasts with solvent extraction studies by Moore *et al.* reporting the formation of solely $NpO_2(Lac)$ up to $[Lac^-]_{tot}$ = 0.1 mol kg_w^{-1}, I_m = 0.3–5.0 mol kg_w^{-1} NaCl and T = 25 °C.[19] This was confirmed by recent solvent extraction studies by Vasiliev *et al.*[18] In contrast to these studies, Inoue *et al.* reported the formation of $NpO_2(Lac)_n^{1-n}$ (n = 1, 2) using absorption spectroscopy and solvent extraction at 1 mol L^{-1} $NaClO_4$, T = 25 °C and $[Lac^-]_{tot}$ = 2.0 mol L^{-1} in the pH_c range of 5.8 to 7.5. These results are in good agreement with those of the present work concerning the stoichiometry of the identified complex species.

3.1.4 Thermodynamic data. Using the experimental speciation data conditional $\log \beta_n'(T)$ values for the formation of $NpO_2(Lac)_n^{1-n}$ (n = 1, 2) are determined at different temperatures and are extrapolated to I_m = 0 with the specific ion interaction theory (SIT) according to eqn (3). Details on the SIT are given elsewhere.[11,12] The extrapolations are given in the ESI† (Fig. S1 and S2).

$$\log \beta' \quad \Delta z^2 D = \log \beta^0 + \Delta \varepsilon I_m \qquad (3)$$

The extrapolated $\log \beta_n^0(T)$ values are summarized in Table 1. At a given temperature the $\log \beta_n^0(T)$ values calculated for NaCl and $NaClO_4$ media are in good agreement within the error range. Hence, averaged values "Ø" for $\log \beta_n^0(T)$ are determined, yielding $\log \beta_1^0$(20 °C) = 1.92 ± 0.09 for $NpO_2(Lac)$ and $\log \beta_2^0$ (20 °C) = 2.10 ± 0.06 for $NpO_2(Lac)_2^-$. With increasing temperature, the first stability constant decreases by 0.12 logarithmic units to $\log \beta_1^0$(85 °C) = 1.80 ± 0.14. The second stability constant decreases by 0.17 logarithmic units to $\log \beta_2^0$(85 °C) = 1.93 ± 0.15. The decrease in the stability constants shows that the complexation of NpO_2^+ with lactate is exothermic. The standard reaction enthalpy $\Delta_r H_{n,m}^0$ and entropy $\Delta_r S_{n,m}^0$ are determined by plotting the averaged $\log \beta_n^0(T)$ *versus* the reciprocal temperature T^{-1}. The data correlate linearly with T^{-1} and the temperature dependence is described by the integrated Van't Hoff equation (eqn (4)) (see Fig. 5).

$$\log \beta_n^0(T) = \log \beta_n^0(T_0) + \frac{\Delta_r H_m^0(T_0)}{R \ln(10)} \left(\frac{1}{T_0} \quad \frac{1}{T} \right) \qquad (4)$$

R is the universal gas constant and T the absolute temperature. T_0 = 298.15 K is the temperature of the IUPAC reference state. The Van't Hoff equation is only valid for a small temperature range of about ΔT = 100 K assuming $\Delta_r C_{m,p}^0$ = 0 and $\Delta_r H_m^0$ = const.

The obtained $\Delta_r H_{n,m}^0$ and $\Delta_r S_{n,m}^0$ values are listed in Table 2 and compared to literature data. The formation of both complexes is slightly exothermic in both electrolytes (NaCl and $NaClO_4$). The averaged standard reaction enthalpies are $\Delta_r H_{1,m}^0(NpO_2(Lac))$ = 4.5 ± 0.5 kJ mol^{-1} and $\Delta_r H_{2,m}^0(NpO_2(Lac)_2^-)$ = 6.0 ± 0.4 kJ mol^{-1}, the standard reaction entropies are $\Delta_r S_{1,m}^0(NpO_2(Lac))$ = 22 ± 5 J mol^{-1} K^{-1} and $\Delta_r S_{2,m}^0(NpO_2(Lac)_2^-)$ = 20 ± 6 J mol^{-1} K^{-1}.

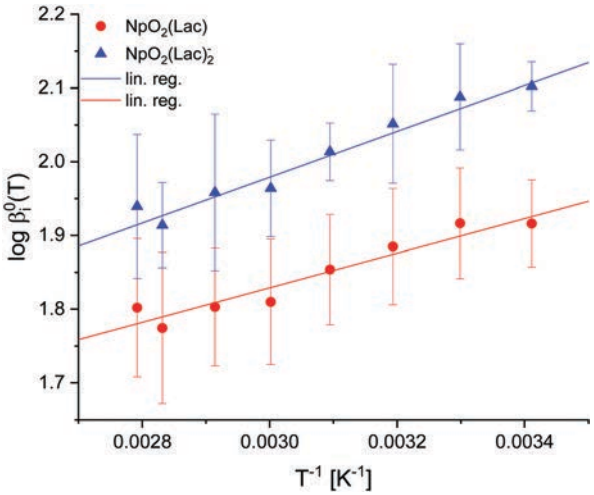

Fig. 5 $\log \beta_n^0(T)$ (n = 1, 2) as a function of the reciprocal temperature and fitting according to the integrated Van't Hoff equation (eqn (4)). Confidence interval: 1 α = 0.95.

In the literature only two $\log \beta_1^0$(25 °C) values are reported determined by solvent extractiontechniques.[19] Moore *et al.* determined $\log \beta_1^0$(25 °C) = 1.70 for the formation of $NpO_2(Lac)$ by application of the SIT and $\log \beta_1^0$(25 °C) = 1.97 by application of the Pitzer model. Both values are in very good agreement with the $\log \beta_1^0$(25 °C) value in the present work. The formation of higher complex species is not described in this survey. A recent study by Vasiliev *et al.* provides a stability constant for $NpO_2(Lac)$ of $\log \beta_1^0$(25 °C) = 1.96 ± 0.05 as well as $\Delta_r H_{1,m}^0$ ($NpO_2(Lac)$)= 5.4 ± 1.4 kJ mol^{-1} and $\Delta_r S_{1,m}^0$ ($NpO_2(Lac)$) = 19 ± 4 kJ mol^{-1}.[18] These results are in excellent agreement with those of the present work. Nevertheless, due to the lower total lactate concentration the formation of higher complex species was not observed by Vasiliev *et al.* In addition, conditional stability constants for $NpO_2(Lac)_n^{1-n}$ (n = 1, 2) determined by Inoue *et al.*, Vasiliev *et al.* and Moore *et al.* at I = 1 mol L^{-1} $NaClO_4$ or NaCl and T = 25 °C are compared to the present work in Table 3.[18–20,51] The spectrophotometrically determined $\log \beta_1'$ by Inoue *et al.* determined from $NaClO_4$ solution is higher compared to the one of the present work whereas the values determined by both solvent extraction studies are significantly lower.

Table 1 Thermodynamic stability constants $\log \beta_n^0(T)$ for the formation of $NpO_2(Lac)_n^{1-n}$ (n = 1, 2) obtained in $NaClO_4$ and NaCl media and their mean values "Ø" as a function of temperature. Confidence interval: 1 α = 0.95. Ø: mean values

	T [°C]	20	30	40	50	60	70	80	85
$[NpO_2(Lac)]$	$NaClO_4$	1.87 ± 0.08	1.88 ± 0.07	1.85 ± 0.09	1.81 ± 0.09	1.76 ± 0.10	1.75 ± 0.05	1.73 ± 0.13	1.73 ± 0.10
	NaCl	1.96 ± 0.06	1.95 ± 0.09	1.92 ± 0.09	1.90 ± 0.08	1.86 ± 0.08	1.85 ± 0.11	1.81 ± 0.09	1.86 ± 0.13
	Ø	1.92 ± 0.10	1.92 ± 0.11	1.88 ± 0.13	1.85± 0.12	1.81 ± 0.13	1.80 ± 0.12	1.77 ± 0.16	1.80 ± 0.16
$[NpO_2(Lac)_2]$	$NaClO_4$	2.04 ± 0.08	2.02 ± 0.09	2.00 ± 0.08	1.96 ± 0.09	1.90 ± 0.12	1.89 ± 0.12	1.86 ± 0.15	1.85 ± 0.15
	NaCl	2.16 ± 0.06	2.15 ± 0.12	2.10 ± 0.15	2.07 ± 0.09	2.03 ± 0.11	2.03 ± 0.15	1.97 ± 0.09	2.02 ± 0.14
	Ø	2.10 ± 0.1	2.09 ± 0.15	2.05 ± 0.17	2.01 ± 0.13	1.96 ± 0.16	1.95 ± 0.19	1.91 ± 0.17	1.93 ± 0.21

Table 2 Thermodynamic functions of the formation of $NpO_2(Lac)_n^{1\ n}$ (n = 1, 2) and comparison to literature data. Confidence interval of the present results: 1 α = 0.95. Ø: mean values. p.w.: present work

Electrolyte	$NpO_2(Lac)_n^{1\ n}$	$\log \beta_n^0$(25 °C)	$\Delta_r H_{n,m}^0$ [kJ mol ^{1}]	$\Delta_r S_{n,m}^0$ [J mol ^{1} K ^{1}]	$\Delta\varepsilon$	Ref.
$NaClO_4$	n 1	1.87 ± 0.11	4.2 ± 0.3	19 ± 4	0.09 ± 0.02	p.w.
	n 2	2.03 ± 0.12	5.8 ± 0.5	22 ± 5	0.20 ± 0.03	p.w.
NaCl	n 1	1.96 ± 0.11	4.8 ± 0.4	21 ± 4	0.12 ± 0.02	p.w.
	n 2	2.15 ± 0.13	6.2 ± 0.3	22 ± 3	0.23 ± 0.02	p.w.
Ø	n 1	1.92 ± 0.14	4.5 ± 0.5	22 ± 5		p.w.
	n 2	2.10 ± 0.13	6.0 ± 0.4	20 ± 6		p.w.
NaCl	n 1	1.96 ± 0.05	5.4 ± 1.4	19 ± 4	0.13 ± 0.03	18
NaCl	n 1	1.70 1.97				19

Table 3 Conditional stability constants for the complexation of NpO_2^+ with lactate at I_m = 1.0 mol kg_w^{-1} and $NaClO_4$ or NaCl as background electrolyte. T = 25 °C

Method	Electrolyte	$\log \beta_{01}'$	$\log \beta_{02}'$	Ref.
A	$NaClO_4$	1.11 ± 0.08	1.78 ± 0.03	20
B	$NaClO_4$	1.09	1.60	51
sp	$NaClO_4$	1.75		20
sp	$NaClO_4$	1.48 ± 0.08	1.77 ± 0.09	p.w.
C	NaCl	1.43 ± 0.04		19
A	NaCl (0.83 mol kg ^{1})	1.75 ± 0.03		18
sp	NaCl	1.67 ± 0.10	1.98 ± 0.11	p.w.

A: solvent extraction with thenoyl trifluoroacetone (TTA) and 1,10 phenantroline (Phen); organic diluent: iso butylmethyl ketone. B: solvent extraction with TTA and alkylammonium; organic diluent: benzene. C: solvent extraction with HDEHP; organic diluent *n* heptane. sp: spectro photometry. p.w.: present work.

Furthermore, different complex species were identified by Inoue *et al.* within the different experimental approaches.[20,51] The solvent extraction experiments reveal the formation of $NpO_2(Lac)_n^{1-n}$ (n = 1, 2), while the spectroscopic study suggests the exclusive formation of $NpO_2(Lac)$. This might explain the huge deviations of the $\log \beta_1'$ values obtained by Inoue *et al.* with the two different experimental methods. The $\log \beta_1'$ by Vasiliev *et al.* is in good agreement to the present result obtained from NaCl solution whereas the value reported by Moore *et al.* is significantly lower.

Furthermore, comparison of the present results with results on the complexation of NpO_2^+ with the structurally related carboxylate ''propionate'' reveals the effect of the α-OH group on the thermodynamic functions. Solvent extraction studies by Vasiliev *et al.* report $\log \beta_1^0(NpO_2(Prop)$, 25 °C) = 1.19–1.26, $\Delta_r H_{1,m}^0$ ($NpO_2(Prop)$) = 10.9–16.3 kJ mol^{-1} and $\Delta_r S_{1,m}^0$ ($NpO_2(Prop)$) = 62–77 J mol^{-1} K^{-1}.[18,22] Comparison with the present results for $NpO_2(Lac)$ shows that the additional α-OH group results in an increase of the complex stability accompanied with a lowering of $\Delta_r H_{1,m}^0$. This points to significant differences in the coordination mode of both ligands. Propionate coordinates end-on towards NpO_2^+ whereas lactate can form chelate complexes involving the COO^- and OH group. A comparison with other simple carboxylates containing α-OH groups (*e.g.* malate or tartrate) is not possible as literature data for NpO_2^+ complexes are not available.

The application of the SIT yields the stoichiometric sum of the binary ion–ion interaction coefficients $\Delta\varepsilon_{j,k}$ of the complex formations. In Fig. 6 the determined $\Delta\varepsilon_{01}$ and $\Delta\varepsilon_{02}$ values are displayed as a function of the temperature for the reaction $NpO_2^+ + nLac^- \rightleftharpoons NpO_2(Lac)_n^{1-n}$ (n = 1, 2) in $NaClO_4$ and NaCl media. No temperature dependence of the $\Delta\varepsilon_{j,k'}$ values is observed in $NaClO_4$. In NaCl $\Delta\varepsilon_{01}$ increases slightly whereas $\Delta\varepsilon_{02}$ remains constant. However, the temperature dependence is negligible within the error range of the data. Various studies on the ionic strength dependence of complexation reactions of trivalent lanthanides and actinides showed, that the effect of temperature on $\Delta\varepsilon_{j,k}$ is rather small and thus negligible in the temperature range of 20 to 90 °C.[22,50,52] Recent studies on the complexation of Np(v) with sulphate, fluoride, formate and acetate support these observations.[43–45,53] Thus, temperature independent $\Delta\varepsilon_{j,k}$ values are calculated for $NaClO_4$ and NaCl media (see Table 2). The averaged values are $\Delta\varepsilon_{01}(NaClO_4)$ = 0.09 ± 0.02, $\Delta\varepsilon_{01}$(NaCl) = 0.12 ± 0.02 and $\Delta\varepsilon_{02}(NaClO_4)$ = 0.20 ± 0.03, $\Delta\varepsilon_{02}$(NaCl) = 0.23 ± 0.02. Comparison with the results by Vasiliev *et al.* ($\Delta\varepsilon_{01}$(NaCl) = 0.13 ± 0.03) shows an excellent agreement with $\Delta\varepsilon_{01}$(NaCl) of the present work. Thus, the ionic strength dependence as a function of the NaCl concentration is accurately described in both studies.

In order to derive the binary ion–ion interaction coefficients $\varepsilon_{j,k}$ of the different NpO_2^+ lactate complexes with both background electrolytes the following parameters stated in the literature are used: $\varepsilon(Na^+, Lac^-)$ = 0.01 ± 0.05, $\varepsilon(NpO_2^+, ClO_4^-)$ = 0.25 ± 0.05 and $\varepsilon(NpO_2^+, Cl^-)$ = 0.09 ± 0.05.[11,48] The $\varepsilon(Na^+ + Cl^-/ClO_4^-, NpO_2(Lac))$ and $\varepsilon(Na^+, NpO_2(Lac)_2^-)$ values are calculated according to eqn (5).

$$\Delta\varepsilon = \sum \varepsilon_{\text{products}} \quad \sum \varepsilon_{\text{educt}} \tag{5}$$

The SIT binary ion–ion interaction parameters for $NpO_2(Lac)$ are $\varepsilon(Na^+ + ClO_4^-, NpO_2(Lac))$ = 0.17 ± 0.05 and $\varepsilon(Na^+ + Cl^-, NpO_2(Lac))$ = 0.02 ± 0.05. For $NpO_2(Lac)_2^-$ the parameters are $\varepsilon(Na^+, NpO_2(Lac)_2^-)$ = 0.07 ± 0.05 determined in $NaClO_4$ and $\varepsilon(Na^+, NpO_2(Lac)_2^-)$ = 0.12 ± 0.05 determined in NaCl. The similarity of $\varepsilon(Na^+ + ClO_4^-, NpO_2(Lac))$ and $\varepsilon(Na^+, NpO_2(Lac)_2^-)$ determined in $NaClO_4$ as well as of $\varepsilon(Na^+ + Cl^-, NpO_2(Lac))$ and $\varepsilon(Na^+, NpO_2(Lac)_2^-)$ determined in NaCl is expected as the observed ionic strength dependence of the respective $\log \beta_n'(T)$ is weak. According to the SIT it is assumed that $\varepsilon_{j,k}$ = 0 for uncharged species. Taking into account the error of the $\varepsilon_{j,k}$ values, this is the case for $\varepsilon(Na^+ + Cl^-, NpO_2(Lac))$. However, $\varepsilon(Na^+ + ClO_4^-, NpO_2(Lac))$ deviates significantly from zero and the

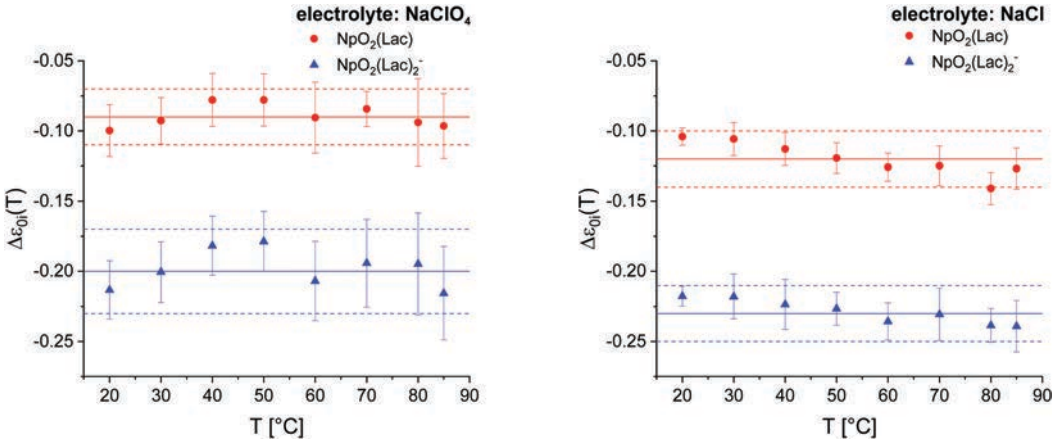

Fig. 6 $\Delta\varepsilon_{j,k}(T)$ values for the reaction $NpO_2^+ + n\text{Lac} \rightleftharpoons NpO_2(Lac)_n^{1-n}$ (n = 1, 2) in $NaClO_4$ (left) and NaCl (right) as a function of the temperature. The error of the mean value (solid line) is represented by the dashed lines.

discrepancy between these two values accounts for 0.19. Similar deviations were observed for the complexes of NpO_2^+ with formate, acetate, fluoride and chloride in $NaClO_4$ media.[43,45,46,53] Furthermore, a comparable deviation is observed for $\varepsilon(Na^+, NpO_2(Lac)_2^-)$ determined in NaCl and $NaClO_4$ media which is also 0.19. Thus, we assume that the $\varepsilon(NpO_2^+, ClO_4^-) = 0.25 \pm 0.05$ given in the NEA-TDB might be defective and should be re-evaluated. Nonetheless, the thermodynamic functions ($\log \beta_n^0(T)$, $\Delta_r H_{n,m}^0$, $\Delta_r S_{n,m}^0$) obtained for both electrolytes (NaCl and $NaClO_4$) are in excellent agreement and thus the ionic strength dependence of the complex formations is accurately described in the present work.

Comparison of the present $\varepsilon_{j,k}$ values determined in NaCl with literature data for the acetate and propionate complexes shows that the ion–ion interaction parameters are all close to zero:[18,22]

$$\varepsilon(Na^+ + Cl^-, NpO_2(Lac)) = 0.05 \pm 0.05$$

$$\varepsilon(Na^+, NpO_2(Lac)_2^-) = 0.02 \pm 0.05$$

$$\varepsilon(Na^+ + Cl^-, NpO_2(Ac)) = 0.02 \pm 0.06$$

$$\varepsilon(Na^+, NpO_2(Ac)_2^-) = \quad 0.01 \pm 0.06$$

$$\varepsilon(Na^+ + Cl^-, NpO_2(Prop)) = 0.03 \pm 0.04$$

$$\varepsilon(Na^+ + Cl^-, NpO_2(Prop)) = 0.00 \pm 0.04$$

Thus, the ionic strength dependence of the formation of the $NpO_2(L)$ and $NpO_2(L)_2^-$ complexes with lactate, acetate and propionate is weak and comparable for all ligands discussed.

3.2 Structural characterization of the $NpO_2(Lac)_n^{1-n}$ complexes

For α-hydroxy carboxylates two coordination modes towards the NpO_2^+ ion are possible (see Scheme 1). Information on the structure of the $NpO_2(Lac)_n^{1-n}$ complexes should show if the α-OH group is involved in the complexation of An(v) ions and how this might affect the thermodynamic behaviour.

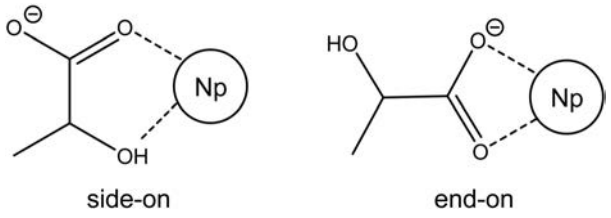

Scheme 1 Possible coordination modes of lactate towards the NpO_2^+ center. (left) side on coordination with a monodentate binding of the COO group, (right) end on coordination with a bidentate binding of the COO group.

3.2.1 EXAFS spectroscopy. The k^2-weighted Np-L_3-edge EXAFS spectra of NpO_2^+ in the presence of lactate, the Fourier transformations and the corresponding fit curves are given in the ESI† in Fig. S3 as a function of the pH_c value. The results of the fits and the fit parameters are listed in Table S1 in the ESI.† A summary of the obtained structural parameters is given in Table 4. The spectra are dominated by the axial and equatorial O-atoms (O_{ax}, O_{eq}). The averaged distance of the axial O-atoms (O_{ax}) is 1.84 ± 0.01 Å and of the equatorial O-atoms (O_{eq}) 2.49 ± 0.02 Å. The coordination number of the NpO_2^+ ion in the equatorial plane varies between 3.1 and 4.9. Both, the coordination numbers and the distances of the O-atoms are not affected by the pH_c value. Furthermore, the results are in excellent agreement with literature data.[54,55]

Table 4 Structural parameters for the $NpO_2(Lac)_n^{1-n}$ (n = 1, 2) complexes obtained from the fits of the raw k^2 weighted Np L_3 edge EXAFS spectra shown in Fig. S3 (ESI)

	pH	0.8	2.6	3.3	4.0	4.7	5.2
O_{ax}	N	2[a]	2[a]	2[a]	2[a]	2[a]	2[a]
	R/Å	1.83 (1)	1.85 (1)	1.83 (1)	1.84 (1)	1.84 (1)	1.84 (1)
O_{eq}	N	4.9 (1)	3.1 (1)	4.2 (1)	4.1 (1)	4.2 (1)	4.1 (1)
	R/Å	2.48 (1)	2.51 (2)	2.49 (1)	2.49 (1)	2.48 (1)	2.48 (1)
C_{coord}	N		1.3 (1)	1.1 (1)	1.2 (1)	1.3 (1)	2.5 (1)
	R/Å		2.72 (8)	2.81 (4)	3.12 (4)	3.14 (2)	3.23 (2)

[a] Fixed for fitting.

The coordination mode of the lactate molecules towards the NpO_2^+ ion is determined by evaluating the distances of the carbon atoms of the coordinating functional groups (–COO^- and –COH). At pH_c = 0.8 no lactate complexes are formed and the spectrum corresponds to the solvated NpO_2^+ ion. At pH_c = 2.6 the evaluation of the EXAFS spectrum reveals 1.3 carbon atoms C_c at 2.72 ± 0.08 Å from the Np(v) center. With increasing pH_c up to 5.2 both, the number of carbon atoms and the C_c distance increase from 1.3–2.5 and from 2.72 ± 0.08–3.23 ± 0.02 Å, respectively. This indicates a change of the coordination mode of lactate with increasing basicity.

Takao *et al.* studied the complexation of NpO_2^+ with acetate by EXAFS spectroscopy.[56] In this study a C_c distance of 2.91 ± 0.02 Å between the NpO_2^+ center and the coordinating COO^- group is reported. In an EXAFS study on Np-propionate complexes by Vasiliev *et al.* a C_c distance of 2.87 ± 0.03 Å was determined.[22] These distances obtained for monocarboxylic ligands serve as reference for an end-on coordination mode of the COO^- group *via* the two O-atoms. Furthermore, the C_c distances obtained for NpO_2^+ complexes are in good agreement with structural parameters of Am(III)-acetate complexes.[57] There, a C_c distance of 2.82 ± 0.05 Å to the americium ion was determined. Literature data on structural parameters of Am(III) lactate complexes show, that the distal C_c atoms are located at 3.42 ± 0.03 A.[47] This is distinctively larger compared to the distance in the Am(III) acetate complexes and indicates a side-on coordination of lactate with the formation of a five-membered chelate ring at $pH_c \geq 3.0$.

The comparison with the known C_c distances for side-on and end-on coordination indicates that at low pH_c lactate coordinates only *via* the COO^--group towards NpO_2^+. With increasing pH_c the C_c distance increases and the coordination mode changes to a side-on coordination of lactate *via* the COO^-- and COH-group. Thus, the proton concentration has a major effect on the coordination mode of lactate towards the NpO_2^+ ion.

3.2.2 ATR FT-IR spectroscopy. The vibrational modes of the coordinated ligand and the NpO_2^+ ion provides additional information on the structure of the complexes and the coordination mode of lactate towards the NpO_2^+ ion.

Prior to the measurement of the NpO_2^+ lactate samples, the vibrational spectra of the pure ligand at identical experimental conditions are recorded (Fig. 7, top). All spectra are dominated by bands at 1716, 1587 and 1416 cm^{-1} representing the vibrational modes of the COOD group as well as the symmetric ($\nu_s(COO^-)$) and anti-symmetric ($\nu_{as}(COO^-)$) modes of the COO^- group. The absorption bands at 1462 and 1116 cm^{-1} corresponds to the ν_{AL}(OH) and ν_{AL}(CO) modes of the COH group. These values are in good agreement with literature data.[58,59]

The infrared spectra of the NpO_2^+ lactate species at various pD_c values (pD_c = 2.6, 4.1, 4.8) are shown in Fig. 7 (bottom) as difference spectra after subtraction of the spectra of the pure ligand. The absorption spectra show a contribution of the free lactic acid which is represented by the negative absorption band at 1716 cm^{-1}. Modes of the ligand undergoing alterations upon complexation are detected as positive absorption bands at 1587, 1456, 1416 and 1100 cm^{-1}.

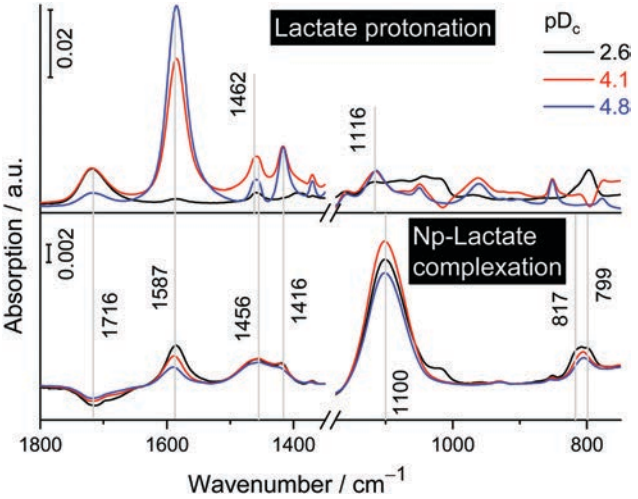

Fig. 7 ATR FT infrared spectra of the lactate protonation and deprotonation (top) and the difference spectra of the NpO_2^+ lactate samples (bottom) as a function of the pD_c value. I_m(NaCl) = 1.0 mol kg_w^{-1}, T = 20 °C, $[NpO_2^+]_{total}$ = 2.0 × 10^{-3} mol kg_w^{-1}, $[Lac^-]_{total}$ = 0.1 mol kg_w^{-1}.

The vibrational band of the $\nu_3(NpO_2)$ mode is observed in the spectral region below 850 cm^{-1}.[24] Its frequency and shape changes slightly as a function of the pD_c value. Thus, a deconvolution of this band was performed, and frequencies of single species were obtained from second derivative spectra (data not shown). At pD_c = 2.6, two bands at 799 and 817 cm^{-1} are observed. The first one represents the OD mode of the free lactate. The band at 817 cm^{-1} is assigned to the free NpO_2^+ ion.[24,60] Thus, at pD_c = 2.6 the NpO_2^+ aquo ion is the predominant species. An increasing number of coordinated lactate molecules in the equatorial plane of the NpO_2^+ ion lowers the frequency of the antisymmetric stretching vibration. Consequently, upon increasing the pD_c value to 4.1 a vibrational band at 804 cm^{-1} is obtained corresponding to a single species, NpO_2Lac. This band remains unchanged in the spectrum obtained at pD_c = 4.8. Thus, the frequency of the $\nu_3(NpO_2)$ mode provides information on the number of different complex species but no direct indication of the coordination mode of the ligand.

However, information on the coordination mode of the ligand to the NpO_2^+ ion can be derived from the antisymmetric and symmetric stretching modes of the carboxylic groups ($\nu_{as}(COO^-)$ and $\nu_s(COO^-)$). Their spectral splitting ($\Delta\nu_{COO}$) allows a differentiation between bidentate and monodentate coordination of the COO^- group to the metal ion.[61,62] Generally, a bidentate coordination is characterized by a smaller splitting ($\Delta\nu_{COO} \leq 100$ cm^{-1}) whereas a monodentate binding results in a larger spectral splitting ($\Delta\nu_{COO} \geq 150$ cm^{-1}).[62] The vibrational modes of the COO^- group of the lactate ligand have nearly the same frequency values throughout the whole pD_c range investigated, that are 1587 cm^{-1} for the $\nu_{as}(COO^-)$ and 1416 cm^{-1} for the $\nu_s(COO^-)$ mode. Therefore, the constant value $\Delta\nu_{COO}$ of about 171 cm^{-1} suggests a monodentate coordination of the COO^- group in the series of the NpO_2^+ lactate spectra excluding an end-on coordination of the ligand towards the

NpO_2^+ ion (compare Scheme 1). Furthermore, the comparison of the spectral data shown in Fig. 7 (top) and (bottom) reveals that the impact of replacing the monovalent Na^+ by NpO_2^+ on the vibrational modes of the COO^- group is not significant. In contrast, a shift of the alcoholic ν_{AL}(CO) band from 1116 to 1100 cm^{-1} and of ν_{AL}(OH) from 1462 to 1456 cm^{-1} is observed indicating that the COH group is involved in the binding of lactate towards NpO_2^+.[58] This shift is unaffected by the pD_c value. According to the EXAFS results with increasing pH_c/pD_c a change of the coordination mode from side-on to end-on is expected. This is not observed by infrared spectroscopy as these results suggest a side-on coordination within the entire pD_c range studied. However, the results of the IR measurements at $pD_c \geq 4.1, 4.8$ are in good agreement with the results obtained by EXAFS for $pH_c \geq 4.0$ indicating a side-on coordination of lactate towards the NpO_2^+ ion.

3.2.3 Quantum chemical calculations. The molecular structures of different constitution isomers of the $NpO_2(Lac)$ and $NpO_2(Lac)_2^-$ complexes (see Scheme 2) are optimized on DFT level using the BH-LYP functional and def-TZVP basis sets.[35–37] A detailed visualization of the structures is given in Fig. S5–S7 in the ESI.† The cartesian coordinates of the optimized complex structures are also given there. The calculated averaged distances of the coordination shells containing the axial O-atoms O_{ax}, the equatorial O-atoms O_{eq} and the C-atoms C_c of the coordinating COO^- and COH group are summarized in Table 5 and compared to the results of the EXAFS evaluation. The data show that the coordination shell distances of the axial and equatorial O-atoms (O_{ax}, O_{eq}) are not affected by the coordination mode of the ligand. Thus, it is not possible to differentiate between the coordination modes of the lactate molecule using the distances of O_{ax} or O_{eq} towards the NpO_2^+ center. However, the average distances of the C_c coordination shell of the COO- and COH-group differ significantly for end-on and side-on coordination. For end-on coordinated lactate a C_c distance of 2.91 Å is calculated which is about 0.48 Å shorter compared to the C_c distance of the side-on coordinated ligand molecule (C_c = 3.39 Å).

The comparison with the experimentally obtained distances shows that the calculated values for O_{ax} and O_{eq} are in excellent agreement with the experimental results. However, the C_c distance determined by EXAFS spectroscopy increase with increasing pH_c from 2.98 up to 3.38 Å. The distance at low pH_c is in good agreement with the calculated distance for the end-on coordinating lactate. The experimentally determined C_c distance at pH_c = 4.9 agrees with the distance for the side-on coordinating lactate *via* the COO^- and COH group. Unfortunately, the quantum chemical calculations do not account for pH_c effects. Nevertheless, the calculations confirm the experimentally observed C_c distances for the end-on and the side-on coordination mode of lactate.

Table 5 Averaged distances of the O_{ax}, O_{eq} and C_c shell towards the metal centre. Experimental EXAFS results and quantum chemical calculations

Method	Complex	Coord. mode	O_{ax} [Å]	O_{eq} [Å]	C_c [Å]
DFT	$NpO_2(Lac)$	End on	1.83	2.49	2.91
		Side on	1.84	2.46	3.39
	$NpO_2(Lac)_2$	End on	1.81	2.47	2.92
		Side on	1.84	2.45	3.39
		Mixed	1.84	2.47	2.86/3.40
EXAFS	$NpO_2(Lac)$/ $NpO_2(Lac)_2$		1.84	2.47	2.72 3.32

Calculations of the Gibb's free energies ΔG provide additional information on the coordination mode of lactate towards NpO_2^+. The Gibb's energies for the isomerisation of $NpO_2(Lac)_n^{1-n}$ (n = 1, 2) are calculated according to eqn (6a)–(6c).

$$NpO_2(Lac)_{(End\text{-}on)} \rightleftharpoons NpO_2(Lac)_{(Side\text{-}on)} \quad (6a)$$

$$NpO_2(Lac)_{2(End\text{-}on)}^- \rightleftharpoons NpO_2(Lac)_{2(Side\text{-}on)}^- \quad (6b)$$

$$NpO_2(Lac)_{2(mixed)}^- \rightleftharpoons NpO_2(Lac)_{2(Side\text{-}on)}^- \quad (6c)$$

ΔG is calculated using the difference of the ground state energies ΔE_g on MP2 level while thermodynamic corrections ΔG_{vib} and solvation effects ΔG_{COSMO} are considered: $\Delta G = \Delta E_g + \Delta G_{vib} + \Delta G_{COMSO}$. The results show, that in case of the isomerisation of $NpO_2(Lac)$ ΔG is positive, whereas it is negative for $NpO_2(Lac)_2^-$ (see Table 6). Thus, for the 1 : 1 complex the end-on coordination of the ligand is more stable compared to the side-on coordination. In contrast, for the 1 : 2 complex the formation of chelate complexes is energetically preferred. Furthermore, the 1 : 2 complex with two lactate molecules forming chelate rings is more stable compared to the mixed structure (see Scheme 2). This is expressed by the more negative ΔG value for the isomerisation according to eqn (6b) in comparison to eqn (6c).

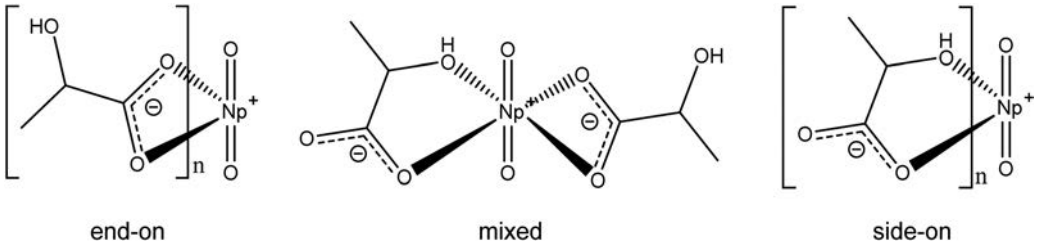

Scheme 2 Schematic structures of the different constitution isomers of the NpO_2^+ lactate complexes. The stoichiometric sum of the complexes in the first coordination sphere is $NpO_2(H_2O)_3(Lac)$ and $NpO_2(H_2O)(Lac)_2$. The second coordination sphere consists of 28 water molecules. The water molecules are omitted for clarity.

Table 6 Gibbs free energies ΔG for the isomerisation of $NpO_2(Lac)_n^{1-n}$ (n = 1, 2) according to eqn (6a)–(6c). Ground state energies calculated on MP2 level

Complex	ΔE_g [kJ mol^{-1}]	ΔG_{vib} [kJ mol^{-1}]	ΔG_{COMSO} [kJ mol^{-1}]	ΔG [kJ mol^{-1}]	Eqn.
$NpO_2(Lac)$	4.20	20.15	6.01	39.89	(6a)
$NpO_2(Lac)_2$	28.13	28.26	18.58	18.71	(6b)
	28.90[a]	1.11[a]	23.85[a]	3.93[a]	(6c)

[a] ΔE $\Delta E_{Side\text{-}on}$ ΔE_{mixed}; ΔG $\Delta G_{Side\text{-}on}$ ΔG_{mixed}.

Table 7 Relative shifts of the calculated vibrational frequencies of the different constitution isomers of the $NpO_2(Lac)$ and $NpO_2(Lac)_2$ complexes from DFT and comparison with the results by FT-IR spectroscopy. $\Delta\nu_{COO} = \nu_{as}(COO^-) - \nu_s(COO^-)$

Complex	Coordination mode	$\nu_{as}(COO^-)$ [cm^{-1}]	$\nu_s(COO^-)$ [cm^{-1}]	$\Delta\nu_{COO}$ [cm^{-1}]
$NpO_2(Lac)$	End-on	1686	1598	88
	Side-on	1730	1457	273
$NpO_2(Lac)_2$	End-on	1676	1569	107
	Side-on	1728	1457	271
	Mixed	1679	1587	92
		1702	1478	224
Exp.	pH 2.6–4.8	1587	1419	171

As vibrational frequencies are calculated to estimate ΔG_{vib} the theoretical spectral shifts $\Delta\nu_{COO} = \nu_{as}(COO^-) - \nu_s(COO^-)$ for the different constitution isomers of the $NpO_2(Lac)$ and $NpO_2(Lac)_2^-$ complexes are compared to the results of the FT-IR spectroscopy in Table 7.

The results of the calculations confirm the interpretation of the FT-IR spectra. For a bidentate coordination of the lactate *via* both O-atoms (end-on) a spectral splitting of $\Delta\nu_{COO} \leq 100$ cm^{-1} is expected. The calculations provide $\Delta\nu_{COO}$ to be 88–107 cm^{-1} for an end-on coordinating lactate. In case of a side-on coordination of lactate $\Delta\nu_{COO} \geq 150$ cm^{-1} is expected.[61,62] The calculations reveal $\Delta\nu_{COO}$ = 224–273 cm^{-1}. In the experiments a value of $\Delta\nu_{COO}$ = 171 cm^{-1} is observed indicating a monodentate coordination of the COO^- group and a side-on coordination of lactate to the NpO_2^+ center.

The quantum chemical calculations do not consider effects of the proton concentration on the coordination mode of lactate. Nevertheless, the results confirm the general trend of changing coordination modes with increasing pH_c observed by EXAFS. An increasing pH_c results in a shift of the chemical equilibrium towards the $NpO_2(Lac)_2^-$ complex, which is in very good agreement to the experimental results, revealing a preferred side-on coordination at higher pH_c values.

4 Summary

In the present work the thermodynamics and structures of the complexes of NpO_2^+ with lactate are investigated by different techniques such as absorption spectroscopy, EXAFS spectroscopy, ATR-FT infrared spectroscopy and quantum chemical calculations. The formation of the NpO_2^+ lactate complexes is studied photometrically as a function of the ligand concentration (Lac^-), ionic strength (NaCl and $NaClO_4$) and temperature (20–85 °C). Two different complex species are observed which are identified as $NpO_2(Lac)$ and $NpO_2(Lac)_2^-$. With increasing temperature, the equilibrium of the complex formation shifts towards the NpO_2^+ aquo ion. $\log\beta_1^0(20\ ^\circ C) = 1.92 \pm 0.09$ decreases by 0.12 and $\log\beta_2^0$ (20 °C) = 2.10 ± 0.06 decreases by 0.17 in the temperature range of 20–85 °C. Correlation of $\log\beta_n^0(T)$ with the reciprocal temperature and fitting according to the integrated Van't Hoff equation yield the standard reaction enthalpies ($\Delta_r H_{n,m}^0$) and entropies ($\Delta_r S_{n,m}^0$) of the complexation reactions. Linear regression analyses reveal $\Delta_r H_{1,m}^0 = 4.5 \pm 0.5$ and $\Delta_r H_{2,m}^0 = 6.0 \pm 0.4$ confirming slightly exothermic complexation reactions.

The $\Delta\varepsilon_{01}$ and $\Delta\varepsilon_{02}$ values are determined as a function of temperature for two different ionic media (NaCl and $NaClO_4$). No significant temperature dependence of $\Delta\varepsilon_{01}$ and $\Delta\varepsilon_{02}$ is observed and averaged, temperature independent values are used to determine $\varepsilon_{j,k}$ values of the NpO_2^+–lactate complexes with the two different electrolytes.

Structural investigations of the formed complexes by EXAFS spectroscopy show a change of the coordination mode of lactate towards the NpO_2^+ center when varying the pH_c. With increasing pH_c the distance of the C-atom shell increases indicating a change of the coordination mode from end-on to side-on. Quantum chemical calculations confirm the bond distances determined by EXAFS for end-on and side-on coordination. Theoretical approximations of the Gibbs free energies for the isomerisation of end-on to side-on coordinated ligands show the preference of the end-on coordination for $NpO_2(Lac)$ and of the side-on coordination for $NpO_2(Lac)_2^-$ which agrees to the trend observed by EXAFS spectroscopy as a function of the pH_c. In contrast to the EXAFS results, the ATR-FT infrared spectra show no effect of the proton concentration on the coordination mode but indicate a side-on coordination of lactate for $pD_c > 2.6$.

It is expected that different coordination modes of lactate have a strong impact on the thermodynamic functions ($\log\beta_n^0(T)$, $\Delta_r H_{n,m}^0$, $\Delta_r S_{n,m}^0$) of the NpO_2^+ complexes. Thus, for the determination of thermodynamic functions detailed information on the structure of the complexes and the coordination mode of the ligand are essential. In the present work the absorption spectroscopic studies were performed at pH_c = 4.9. At this pH_c lactate coordinates in the side-on mode forming chelate complexes.

The present work is a detailed study on the complexation of NpO_2^+ with lactate providing thermodynamic data and structural information on the formed complexes. The results highlight the effect of the α-hydroxy group on the thermodynamic functions compared to simple monocarboxylates and the effect of the proton concentration on the coordination mode. Furthermore, the here determined data contribute to the thermodynamic database of actinides improving the scientific basis for understanding the chemical behaviour of pentavalent actinides in the presence of multifunctional organic ligands in aqueous solution.

Conflicts of interest

There are no conflicts to declare.

Acknowledgements

The absorption spectroscopic measurements were carried out at the Institute for Nuclear Waste Disposal (INE) at Karlsruhe Institute of Technology (KIT). Dr D. Fellhauer and Dr M Altmaier are acknowledged for providing the ^{237}Np and comprehensive experimental support. The KIT Institute for Beam Physics and Technology (IBPT) is acknowledged for the operation of the storage ring, the Karlsruhe Research Accelerator (KARA), and provision of beamtime at the KIT light source. The ATR-FT-IR measurements were performed at the Institute of Resource Ecology at the Helmholtz-Zentrum Dresden-Rossendorf (HZDR). Dr H. Foerstendorf is acknowledged for the helpful discussions and support in the data treatment.

This work is supported by the German Federal Ministry for Economic Affairs and Energy (BMWI) under contract 02E11415H and the German Federal Ministry of Education and Research (BMBF) under contract 02NUK039C.

References

1 R. Gens, P. Lalieux, P. D. Preter, A. Dierckx, J. Bel, J.-P. Boyazis and W. Cool, The Second Safety Assessment and Feasibility Interim Report (SAFIR 2 Report) on HLW Disposal in Boom Clay: Overview of the Belgian Programme, *MRS Proc.*, 2011, **807**, 917–924.

2 N. E. A. Oecd, Nuclear Energy Agency Organisation For Economic Co-Operation And Development, *Safety of Geological Disposal of High-level and Long-lived Radioactive Waste in France*, 2006.

3 P. Hoth; H. Wirth; K. Reinhold; V. Bräuer; P. Krull and H. Feldrappe, *Endlagerung radioaktiver Abfälle in tiefen geologischen Formationen Deutschlands–Untersuchung und Bewertung von Tongesteinsformationen*, BGR Bundesanstalt für Geowissenschaften und Rohstoffe, Hannover/Germany, 2007.

4 NAGRA Projekt Opalinuston – Synthese der geowissenschaftlichen Untersuchungsergebnisse, Entsorgungsnachweis für abgebrannte Brennelemente, verglaste hochaktive sowie langlebige mittelaktive Abfälle; NAGRA Nationale Genossenschaft für die Lagerung radioaktiver Abfälle: Wettingen/Switzerland, 2002.

5 K. Mengel, K.-J. Röhlig and H. Geckeis, Endlagerung radioaktiver Abfälle, *Chem. Unserer Zeit*, 2012, **46**(4), 208–217.

6 H. Geckeis, J. Lutzenkirchen, R. Polly, T. Rabung and M. Schmidt, Mineral-water interface reactions of actinides, *Chem. Rev.*, 2013, **113**(2), 1016–1062.

7 E. Gaucher, C. Robelin, J. M. Matray, G. Negral, Y. Gros, J. F. Heitz, A. Vinsot, H. Rebours, A. Cassagnabere and A. Bouchet, ANDRA underground research laboratory: interpretation of the mineralogical and geochemical data acquired in the Callovian-Oxfordian formation by investigative drilling, *Phys. Chem. Earth*, 2004, **29**(1), 55–77.

8 T. R. Allen; R. E. Stoller and S. Yamanaka, *Comprehensive Nuclear Materials*, Elsevier, Radarweg 29, PO Box 211, 1000 AE Amsterdam, The Netherlands, 2012.

9 A. Courdouan, I. Christl, S. Meylan, P. Wersin and R. Kretzschmar, Isolation and characterization of dissolved organic matter from the Callovo–Oxfordian formation, *Appl. Geochem.*, 2007, **22**(7), 1537–1548.

10 A. Courdouan, I. Christl, S. Meylan, P. Wersin and R. Kretzschmar, Characterization of dissolved organic matter in anoxic rock extracts and in situ pore water of the Opalinus Clay, *Appl. Geochem.*, 2007, **22**(12), 2926–2939.

11 R. Guillaumont; T. Fanghänel; V. Neck; J. Fuger and D. A. Palmer, *Update on the Chemical Thermodynamics of Uranium, Neptunium, Plutonium, Americium and Technetium*, Elsvier B.V., 2003.

12 R. J. Lemire, *Chemical thermodynamics of neptunium and plutonium*, Elsevier, 2001, vol. 4.

13 W. Hummel; G. Anderegg; L. Rao; I. Puigdomenech and O. Tochiyama, *Chemical Thermodynamics of Compounds and Complexes of U, Np, Pu, Am, Tc, Se, Ni and Zr with Selected Organic Ligands*, Elsvier B.V., 2005.

14 G. R. Choppin, Actinide speciation in aquatic systems, *Mar. Chem.*, 2006, **99**(1–4), 83–92.

15 G. R. Choppin, Actinide speciation in the environment, *J. Radioanal. Nucl. Chem.*, 2007, **273**(3), 695–703.

16 T. Fanghänel and V. Neck, Aquatic chemistry and solubility phenomena of actinide oxides/hydroxides, *Pure Appl. Chem.*, 2002, **74**(10), 1895–1907.

17 K. Maher, J. R. Bargar and G. E. Brown, Jr., Environmental speciation of actinides, *Inorg. Chem.*, 2013, **52**(7), 3510–3532.

18 A. N. Vasiliev, N. L. Banik, R. Marsac, S. N. Kalmykov and C. M. Marquardt, Determination of complex formation constants of neptunium(v) with propionate and lactate in 0.5–2.6 m NaCl solutions at 22–60 °C using a solvent extraction technique, *Radiochim. Acta*, 2019, **107**(7), 623–634.

19 R. C. Moore, M. Borkowski, M. G. Bronikowski, J. Chen, O. S. Pokrovsky, Y. Xia and G. R. Choppin, Thermodynamic Modeling of Actinide Complexation with Acetate and Lactate at High Ionic Strength, *J. Solution Chem.*, 1999, **28**(5), 521–531.

20 Y. Inoue and O. Tochiyama, Study of the complexes of Np(v) with organic ligands by solvent extraction with TTA and 1, 10-phenanthroline, *Polyhedron*, 1983, **2**(7), 627–630.

21 D. Fellhauer, J. Rothe, M. Altmaier, V. Neck, J. Runke, T. Wiss and T. Fanghänel, Np(v) solubility, speciation and solid phase formation in alkaline $CaCl_2$ solutions. Part I: Experimental results, *Radiochim. Acta*, 2016, **104**(6), 355–379.

22 A. N. Vasiliev, N. L. Banik, R. Marsac, D. R. Fröhlich, J. Rothe, S. N. Kalmykov and C. M. Marquardt, Np(v) complexation with propionate in 0.5–4 M NaCl solutions at 20–85 degrees C, *Dalton Trans.*, 2015, **44**(8), 3837–3844.

23 M. Altmaier, V. Metz, V. Neck, R. Müller and T. Fanghänel, Solid-liquid equilibria of $Mg(OH)_2$(cr) and $Mg_2(OH)_3Cl\cdot 4H_2O$(cr) in the system Mg–Na–H–OH–Cl–H_2O at 25 °C, *Geochim. Cosmochim. Acta*, 2003, **67**(19), 3595–3601.

24 K. Müller, H. Foerstendorf, V. Brendler and G. Bernhard, Sorption of Np(v) onto TiO_2, SiO_2, and ZnO: An *in situ* ATR FT-IR spectroscopic study, *Environ. Sci. Technol.*, 2009, **43**(20), 7665–7670.

25 P. K. Glasoe and F. A. Long, Use of glass electrodes to measure acidities in deuterium oxide, *J. Phys. Chem.*, 1960, **64**(1), 188–190.

26 A. Skerencak, P. J. Panak, V. Neck, M. Trumm, B. Schimmelpfennig, P. Lindqvist-Reis, R. Klenze and T. Fanghänel, Complexation of Cm(III) with fluoride in aqueous solution in the temperature range from 20 to 90 degrees C. A joint TRLFS and quantum chemical study, *J. Phys. Chem. B*, 2010, **114**(47), 15626–15634.

27 A. Skerencak, P. J. Panak, W. Hauser, V. Neck, R. Klenze, P. Lindqvist-Reis and T. Fanghanel, TRLFS study on the complexation of Cm(III) with nitrate in the temperature range from 5 to 200 °C, *Radiochim. Acta*, 2009, **97**(8), 385–393.

28 A. Skerencak, P. J. Panak and T. Fanghänel, Complexation and thermodynamics of Cm(III) at high temperatures: the formation of $[Cm(SO_4)_n]^{3-}2n$ (n = 1, 2, 3) complexes at T = 25 to 200 °C, *Dalton Trans.*, 2013, **42**, 542–549.

29 G. N. George and I. J. Pickering, *EXAFSPAK: A suite of computer programs for analysis of X-ray absorption spectra*, SSRL, Stanford, 1995.

30 B. Ravel and M. Newville, ATHENA, ARTEMIS, HEPHAESTUS: data analysis for X-ray absorption spectroscopy using IFEFFIT, *J. Synchrotron Radiat.*, 2005, **12**(Pt 4), 537–541.

31 M. Newville, IFEFFIT: interactive XAFS analysis andFEFFfitting, *J. Synchrotron Radiat.*, 2001, **8**(2), 322–324.

32 J. J. Rehr, J. J. Kas, M. P. Prange, A. P. Sorini, Y. Takimoto and F. Vila, Ab initio theory and calculations of X-ray spectra, *C. R. Phys.*, 2009, **10**(6), 548–559.

33 Z. V. Akhmerkina, L. B. Serezhkina, V. N. Serezhkin, Y. N. Mikhajlov and Y. E. Gorbunova, Crystal structure of $Ba[UO_2(C_2O_4)_2(H_2O)]\cdot 4H_2O$, *Zhurnal Neorganicheskoj Khimii*, 2004, **49**(10), 1692–1695.

34 A. S. Lermontov, E. K. Lermontova and Y.-Y. Wang, Synthesis, structure and optic properties of 2-methylimidazolium and 2-phenylimidazolium uranyl acetates, *Inorg. Chim. Acta*, 2009, **362**(10), 3751–3755.

35 F. Furche, R. Ahlrichs, C. Hättig, W. Klopper, M. Sierka and F. Weigend, Turbomole, *Wiley Interdiscip. Rev.: Comput. Mol. Sci.*, 2014, **4**(2), 91–100.

36 A. D. Becke, A new mixing of Hartree–Fock and local density-functional theories. *The*, *J. Chem. Phys.*, 1993, **98**(2), 1372.

37 W. Küchle, M. Dolg, H. Stoll and H. Preuss, Energy-adjusted pseudopotentials for the actinides. Parameter sets and test calculations for thorium and thorium monoxide, *J. Chem. Phys.*, 1994, **100**(10), 7535.

38 F. Weigend and M. Häser, RI-MP2: first derivatives and global consistency, *Theor. Chem. Acc.*, 1997, **97**(1–4), 331–340.

39 F. Weigend, M. Häser, H. Patzelt and R. Ahlrichs, RI-MP2: optimized auxiliary basis sets and demonstration of efficiency, *Chem. Phys. Lett.*, 1998, **294**(1–3), 143–152.

40 A. Klamt and G. Schüürmann, COSMO: a new approach to dielectric screening in solvents with explicit expressions for the screening energy and its gradient, *J. Chem. Soc., Perkin Trans. 2*, 1993, 799.

41 Y. Yang, Z. Zhang, G. Liu, S. Luo and L. Rao, Effect of temperature on the complexation of NpO_2^+ with benzoic acid: Spectrophotometric and calorimetric studies, *J. Chem. Thermodyn.*, 2015, **80**, 73–78.

42 Z. Zhang, Y. Yang, G. Liu, S. Luo and L. Rao, Effect of temperature on the thermodynamic and spectroscopic properties of Np(v) complexes with picolinate, *RSC Adv.*, 2015, **5**(92), 75483–75490.

43 M. M. Maiwald, A. Skerencak-Frech and P. J. Panak, The complexation and thermodynamics of neptunium(v) with acetate in aqueous solution, *New J. Chem.*, 2018, **42**(10), 7796–7802.

44 M. M. Maiwald, T. Sittel, D. Fellhauer, A. Skerencak-Frech and P. J. Panak, Thermodynamics of neptunium(v) complexation with sulfate in aqueous solution, *J. Chem. Thermodyn.*, 2018, **116**, 309–315.

45 M. M. Maiwald, D. Fellhauer, A. Skerencak-Frech and P. J. Panak, The complexation of neptunium(v) with fluoride at elevated temperatures: Speciation and thermodynamics, *Appl. Geochem.*, 2019, **104**, 10–18.

46 V. Neck, T. Fanghänel, G. Rudolph and J. I. Kim, Thermodynamics of Neptunium(v) in Concentrated Salt Solutions: Chloride Complexation and Ion Interaction (Pitzer) Parameters for the NpO_2^+ Ion, *Radiochim. Acta*, 1995, **69**(1), 39–47.

47 D. R. Fröhlich, A. Skerencak-Frech, U. Kaplan, C. Koke, A. Rossberg and P. J. Panak, An EXAFS spectroscopic study of Am(III) complexation with lactate, *J. Synchrotron Radiat.*, 2015, **22**(6), 1469–1474.

48 A. Skerencak-Frech, F. Taube, P. L. Zanonato, M. Acker, P. J. Panak and P. Di Bernardo, A potentiometric and microcalorimetric study of the complexation of trivalent europium with lactate: The ionic strength dependency of $\log \beta_n'$, $\Delta_r H_{m,n}$ and $\Delta_r S_{m,n}$, *Thermochim. Acta*, 2019, 679.

49 A. E. Martell; R. M. Smith and R. J. Motekaitis, NIST standard reference database 46 version 8.0: NIST critically selected stability constants of metal complexes. U.S. Department of Commerce, Technology Administration, National Institute of Standards and Technology, Standard Reference Data Program, Gaithersburg, MD, 2004.

50 A. Skerencak-Frech, M. Maiwald, M. Trumm, D. R. Fröhlich and P. J. Panak, The complexation of Cm(III) with oxalate in aqueous solution at T = 20–90 °C: a combined TRLFS and quantum chemical study, *Inorg. Chem.*, 2015, **54**(4), 1860–1868.

51 Y. Inoue, O. Tochiyama and T. Takahashi, Study of the Carboxylate Complexing of Np(v) by Solvent Extraction with TTA and Capriquat, *Radiochim. Acta*, 1982, **31**(3–4), 197–199.

52 D. R. Fröhlich, A. Skerencak-Frech and P. J. Panak, A spectroscopic study on the formation of Cm(III) acetate complexes at elevated temperatures, *Dalton Trans.*, 2014, **43**(10), 3958–3965.

53 M. M. Maiwald, K. Dardenne, J. Rothe, A. Skerencak-Frech and P. J. Panak, Thermodynamics and Structure of Neptunium(v) Complexes with Formate. Spectroscopic and Theoretical Study, *Inorg. Chem.*, 2020, **59**(9), 6067–6077.

54 P. G. Allen, J. J. Bucher, D. K. Shuh, N. M. Edelstein and T. Reich, Investigation of Aquo and Chloro Complexes of

UO22+, NpO2+, Np4+, and Pu3+ by X-ray Absorption Fine Structure Spectroscopy, *Inorg. Chem.*, 1997, **36**(21), 4676–4683.

55 T. Reich, G. Bernhard, G. Geipel, H. Funke, C. Hennig, A. Roßberg, W. Matz, N. Schell and H. Nitsche, The Rossendorf Beam Line ROBL – a dedicated experimental station for XAFS measurements of actinides and other radionuclides, *Radiochim. Acta*, 2000, **88**(9–11), 633–637.

56 K. Takao, S. Takao, A. C. Scheinost, G. Bernhard and C. Hennig, Complex formation and molecular structure of neptunyl(VI) and -(V) acetates, *Inorg. Chem.*, 2009, **48**(18), 8803–8810.

57 D. R. Fröhlich, A. Skerencak-Frech, N. Bauer, A. Rossberg and P. J. Panak, The pH dependence of Am(III) complexation with acetate: an EXAFS study, *J. Synchrotron Radiat.*, 2015, **22**(1), 99–104.

58 G. Cassanas, M. Morssli, E. Fabregue and L. Bardet, Vibrational-spectra of lactic-acid and lactates, *J. Raman Spectrosc.*, 1991, **22**(7), 409–413.

59 M. Hesse; H. Meier and B. Zeeh, *Spektroskopische Methoden in der organischen Chemie. 7. Auflage* ed., Georg Thieme Verlag, 2005.

60 L. H. Jones and R. A. Penneman, Infrared Spectra and Structure of Uranyl and Transuranium(V) and (VI) Ions in Aqueous Perchloric Acid Solution, *J. Chem. Phys.*, 1953, **21**(3), 542–544.

61 G. B. Deacon and R. J. Phillips, Relationships between the carbon-oxygen stretching frequencies of carboxylato complexes and the type of carboxylate coordination, *Coord. Chem. Rev.*, 1980, **33**(3), 227–250.

62 M. Kakihana, T. Nagumo, M. Okamoto and H. Kakihana, Coordination structures for uranyl carboxylate complexes in aqueous-solution studied by IR and C-13 NMR-Spectra, *J. Phys. Chem.*, 1987, **91**(24), 6128–6136.